

0.55T Prostate Diffusion-Weighted Imaging Using Multi-Shot EPI and Self-Supervised Learning Reconstruction

Primary: Diffusion - Diffusion Reconstruction **Secondary:** Acquisition & Reconstruction - Image Reconstruction: AI **Presentation:** Oral, PowerPitch Oral

Keywords: IMAGE RECONSTRUCTION PROSTATE DIFFUSION MRI UNROLLED NETWORKS AND RECONSTRUCTION SELF-SUPERVISED LEARNING

Zhengguo Tan  ¹, **Jacob Richardson**¹, **Thomas L Chenevert**¹, **Hero Hussain**¹, **Michael Jaroszewicz**¹, **Yun Jiang**^{1,2}, **Nicole Seiberlich**^{1,2}, **Vikas Gulani**¹

¹Department of Radiology, University of Michigan, Ann Arbor, MI, United States of America

²Department of Biomedical Engineering, University of Michigan, Ann Arbor, MI, United States of America

 **Presenting Author:** Zhengguo Tan (zhengguo.tan@gmail.com)

Impact

This study supplies a reliable and accurate prostate DWI method at 0.55T, leveraging multi-shot EPI acquisition and self-supervised unrolled joint reconstruction. This method will allow for large cohort prostate patient studies at 0.55T.

Synopsis

Motivation: Clinical prostate diffusion-weighted imaging based on EPI at 0.55T suffers from poor resolution and low signal-to-noise ratio.

Goals: The goal is to develop an acquisition and reconstruction strategy that enables high-resolution prostate DWI at 0.55T.

Approach: This study leverages accelerated multi-shot EPI and ADMM unrolled reconstruction with self-supervised learning.

Results: Our results demonstrate accurate ADC values with 1.6 mm in-plane resolution at 0.55T.

INTRODUCTION

Prostate cancer is the most common cancer in men and one of the leading causes of cancer deaths [1]. Diffusion-weighted imaging (DWI) and its derived apparent diffusion coefficient (ADC) are two key image contrasts for clinical diagnosis and assessment of prostate cancer, according to PI-RADS [2]. Recently, there has been increasing interest in adopting DWI at 0.55T due to reduced field inhomogeneity in the setting of hip implants and rectal gas [3]. However, EPI-based DWI at 0.55T still suffers from poor resolution and low SNR. To address these challenges, this study aims to develop an acquisition and reconstruction strategy leveraging accelerated multi-shot EPI and self-supervised reconstruction unrolling ADMM (alternating direction method of multipliers).

METHODS

Multi-Shot EPI With Repetition-Shifted Encoding

[Figure 1](#) lists acquisition parameters of a clinical single-shot EPI sequence and a proposed multi-shot sequence. The 2-shot interleaved EPI with 4-fold in-plane acceleration per shot reaches 1.6 mm in-plane resolution. In addition, the acquired phase-encoding lines in one repetition are shifted by one line with respect to the preceding repetition, achieving complementary k-q-space sampling [4]. The 3-scan trace diffusion acquisition mode is employed in both protocols. After image reconstruction, trace-weighted images are computed as geometric means of all diffusion-weighted images with the same b-value. Subsequently, the ADC map can be fitted from the following equation:

$$\text{TRACE}_i = b_0 \cdot e^{-b_i \cdot \text{ADC}} \quad (1)$$

Here, i denotes the index of different b-values acquired and b_0 denotes the non-diffusion-weighted spin-echo image. While Protocol #1 uses only three b-values with many averages, we propose using six different b-values but fewer averages for more contrasts.

Scans at 0.55T (FreeMax, Siemens, Erlangen, Germany) were conducted on the caliber diffusion phantom and healthy male subjects with written consent in compliance with IRB.

ADMM Unrolled Self-Supervised Reconstruction

We extend the ADMM unrolled self-supervised reconstruction [5] for prostate DWI at 0.55T. The ADMM unrolled reconstruction formulates a joint k-q-space minimization problem:

$$\operatorname{argmin}_x \|y - \mathcal{A}x\|_2 + \lambda \mathcal{R}(x) \quad (2)$$

where x consists of all diffusion-weighted images. The chained operator \mathcal{A} maps x to the acquired k-space data y through the multiplication of shot-to-shot phase variation, coil sensitivities, Fourier transform, and undersampling patterns. The regularization term $\mathcal{R}(x)$ is represented by the 2D ResNet [6], which is trained via the data splitting mechanism [7,8]. Here, we split y spatially. The model is trained and tested on a A40 GPU with 48 GB memory (NVIDIA, Santa Clara, CA). After reconstruction, ADC maps are computed with MRtrix3.

RESULTS

[Figure 2](#) validates the ADC values using the caliber diffusion phantom. Both protocols supply accurate ADC values. The proposed ADMM unrolling significantly reduces standard deviation of ADC values than parallel imaging as MUSE [9]. Larger standard deviation is seen in Tube 6, because of the low ADC value (i.e., low diffusion contrast-to-noise ratio).

[Figure 3](#) compares the trace-weighted images at the b-value of 500 s/mm^2 . The proposed ADMM unrolling shows significantly reduced noise compared to MUSE and improved spatial resolution compared to the vendor reconstruction.

[Figure 4](#) shows the quantitative ADC maps from both acquisition protocols. While MUSE suffers from severe noise, ADMM unrolling significantly reduces noise and preserves sharp delineation of prostate peripheral zone. A ROI analysis of the central gland shows similar ADC values ($1.3 \times 10^{-3} \text{ mm}^2/\text{s}$) from both protocols. However, the ADC value of the peripheral zone from ADMM unrolling is $1.9 \times 10^{-3} \text{ mm}^2/\text{s}$, higher than Protocol #1 that yields $1.5 \times 10^{-3} \text{ mm}^2/\text{s}$.

[Figure 5](#) displays computed trace-weighted images at the b-value of 1600 s/mm^2 . The vendor reconstruction illustrates blurred boundaries among prostate zones. Our method delivers clear definition of all zones. The central gland shows slightly brighter trace signal than the peripheral zone because of its higher ADC value.

DISCUSSION

This study presents a high in-plane resolution DWI technique at 0.55T based on multi-shot EPI acquisition and ADMM unrolled reconstruction. Clinical prostate DWI based on single-shot EPI renders limited spatial resolution. Spatial interpolation and filtering from the vendor reconstruction shows strong blurring in the computed high b-value trace-weighted images and may be the cause of the reduced ADC value in the peripheral zone. In contrast, our proposed method acquires true 1.6 mm in-plane resolution, and ADMM unrolling effectively reduces noise while preserving sharp delineation of prostate regions.

CONCLUSION

This study develops a high-resolution prostate DWI technique at 0.55T. This technique addresses the challenge of reduced SNR at 0.55T and may serve as a useful tool for prostate imaging in patients for whom 3T imaging is sub-optimal.

References

1. Siegel RL, Giaquinto AN, Jemal A. Cancer statistics, 2024. CA: A Cancer Journal for Clinicians 2024;74:12-49. doi:10.3322/caac.21820
2. Weinreb JC, Barentsz JO, Choyke PL, Cornud F, Haider MA, Macura KJ, et al. PI-RADS Prostate Imaging – Reporting and Data System: 2015, Version 2. European Urology 2016;69:16-40. doi:10.1016/j.eururo.2015.08.052
3. Kelsey LJ, Seiberlich N, Morehouse J, et al. Routine and advanced neurologic imaging at 0.55T MRI: opportunities and challenges. RadioGraphics 2025;45:e240076. doi:10.1148/rg.240076
4. Tan Z, Liebig PA, Heidemann RM, Laun FB, Knoll F. Accelerated diffusion-weighted MRI at 7T: joint reconstruction for shift-encoded navigator-based interleaved EPI (JETS-NAViEPI). Imaging Neuroscience 2024;2:imag-2-00085. doi:10.1162/imag_a_00085
5. Tan Z, Liebig PA, Hofmann A, Laun FB, Knoll F. High-resolution diffusion-weighted imaging with self-gated self-supervised unrolled reconstruction. Magn Reson Med (2025).
6. He K, Zhang X, Ren S, Sun J. Deep residual learning for image recognition. CVPR (2016). doi:10.1109/CVPR.2016.90
7. Yaman B, Hosseini SAH, Moeller S, Ellermann J, Ugurbil K, Akcakaya M. Self-supervised learning of physics-guided reconstruction neural networks without fully sampled reference data. Magn Reson Med 2020;84:3172-3191. doi:10.1002/mrm.28378
8. Yaman B, Hosseini SAH, Akcakaya M. Zero-shot self-supervised learning for MRI reconstruction. ICLR (2022).
9. Chen NK, Guidon A, Chang HC, Song AW. A robust multi-shot scan strategy for high-resolution diffusion weighted MRI enabled by multiplexed sensitivity-encoding (MUSE). NeuroImage 2013;72:41-47. doi:10.1016/j.neuroimage.2013.01.038

Figures and Tables

| Protocol | #1 (2.4 mm) | | #2 (1.6 mm) | |
|-------------------------------|--------------|------|-------------|-----------------------------|
| FOV (mm) | 240 | | | |
| Base resolution | 106 | | 150 | |
| Phase resolution (%) | 65 | | 100 | |
| Slice thickness (mm) | 4 | | 5 | |
| Slices | 15 | | 9 | |
| Diffusion mode | 3-scan trace | | | |
| b-values (s/mm ²) | 50, | 500, | 800 | 50, 100, 200, 300, 400, 500 |
| Averages | 3, | 12, | 27 | 2, 2, 4, 6, 8, 12 |
| Shots | 1 | | 2 | |
| Acceleration | 3 | | 2 | |
| Partial Fourier | 7/8 | | 5/8 | |
| TE/TR (ms) | 92/3900 | | 71/2400 | |
| Acquisition (min) | 8:26 | | 8:16 | |



Scan for high-resolution version

Figure 1: 0.55T prostate DWI acquisition protocols.

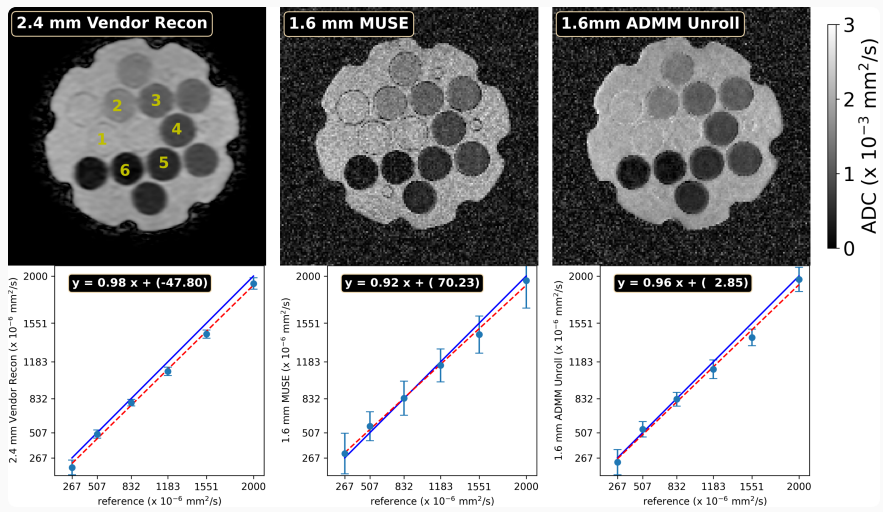


Figure 2: ADC validation using the caliber diffusion phantom. (Top) reconstructed ADC maps from both protocols. (Bottom) region-of-interest analysis of ADC values in the marked tubes.

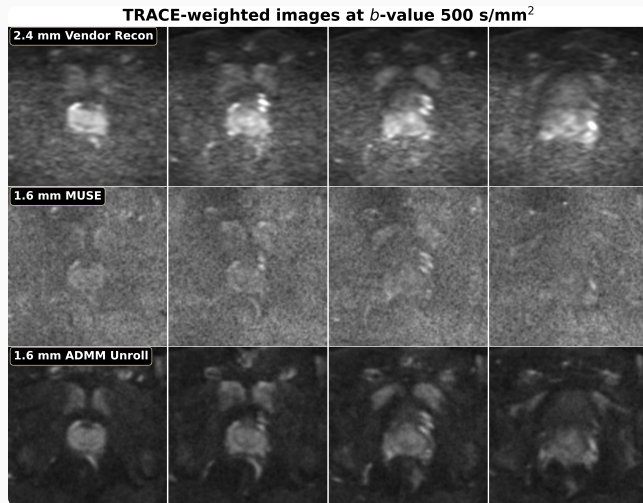
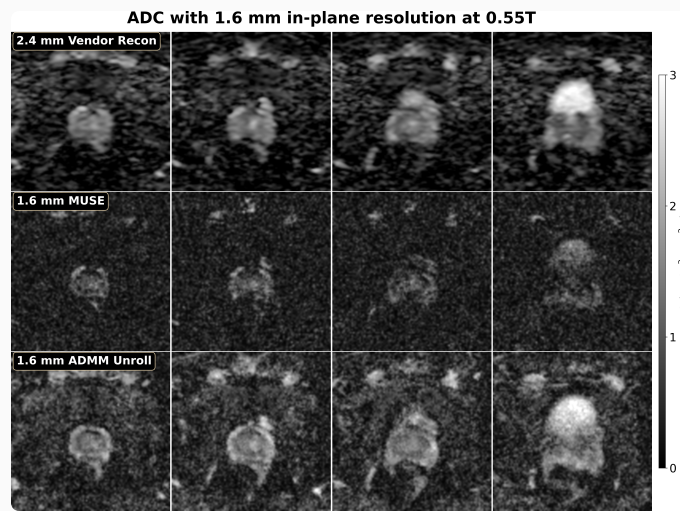


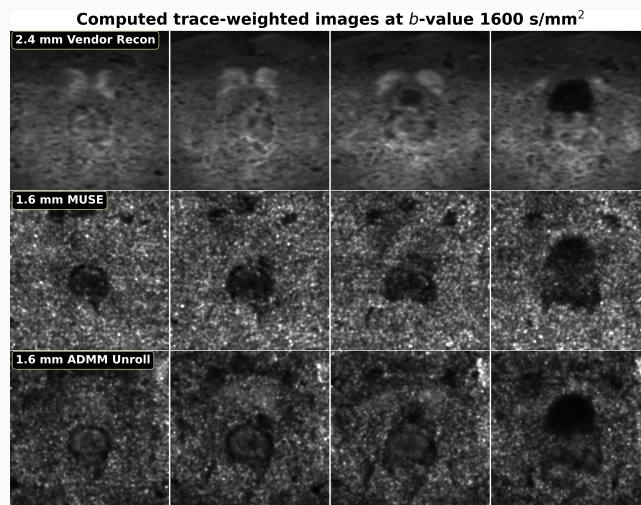
Figure 3: Comparison of trace-weighted images at the b -value of 500 s/mm^2 : (top) Protocol #1 with 2.4 mm vendor reconstruction (deep resolve), (middle and bottom) Protocol #2 with 1.6 mm reconstructed by MUSE and ADMM unrolling, respectively.





Scan for high-resolution version

Figure 4: ADC maps from (top) 2.4 mm in-plane resolution and vendor online reconstruction (Protocol #1), (middle and bottom) 1.6 mm in-plane resolution (Protocol #2) with MUSE and ADMM unrolled reconstruction, respectively.



Scan for high-resolution version

Figure 5: Computed trace-weighted images at the b -value of 1600 s/mm².

